Adhesion between a thin elastic plate and a hard randomly rough substrate

G. Carbone,[1,2] L. Mangialardi,[1] and B. N. J. Persson[2]
[1]*DIMeG-Politecnico di Bari, V.le Japigia 182, 70126 Bari-Italy*
[2]*IFF Forschungszentrum Jülich, 52425 Jülich, Germany*
(Received 16 March 2004; published 13 September 2004)

In this paper we discuss the adhesion of a thin elastic plate to a randomly rough hard substrate. It is shown that at small magnification (long length scales) the plate, because of its higher compliance, is able to adhere in apparent full contact to the long wavelength corrugation of the underlying surface. That is, at length scales longer than the plate thickness, the gain in the adhesion energy upon the contact with the substrate overcomes the repulsive elastic energy produced by the elastic deformations, and the plate is able to fill out the large cavities of the rigid substrate. This produces a larger area of contact and an enhanced capability to adhere to a rough surface in comparison to the semi-infinite elastic solid case. However, at large enough magnification (small length scales) the plate behaves as a semi-infinite solid, and, depending on the roughness statistical properties, the area of true atomic contact may be much smaller than the nominal contact area.

DOI: 10.1103/PhysRevB.70.125407 PACS number(s): 81.40.Pq, 62.20.−x

I. INTRODUCTION

The interaction between two contacting surfaces at the nanoscale is fundamental for many modern high-tech applications, e.g. electromechanical devices,[1] and in biological systems.[2] In particular, adhesion may be deleterious in micro- and nano-devices, e.g. in electromechanical switchers that can fail because of the permanent adhesion of their moving components.[3] On the other hand, in some cases, adhesion may be beneficial, as for thin films used as protective coatings,[4] for the manufacturing of multilayered wafer structures,[6] or in bio-films for orthopedic implants.[5] Since the area of real contact is largely influenced by adhesion,[7] it is of direct importance also for sliding friction,[8–14] and it will influence the contact resistivity and the heat transfer between the solids. In previous papers[9,15] we have studied the problem of a semi-infinite elastic solid in adhesive partial contact with a rigid profile with "roughness" on a single length scale. For this system the effective adhesion energy,[15] and the forces for jump into contact and jump out of contact have been evaluated.[9] The problem of partial contact between a semi-infinite elastic solid and a randomly rough profile has been studied in Ref. 7, and in Ref. 16 one of us has studied the contact between elastic plates and a hard substrate with "roughness" on a single length scale. These works have shown that, for very soft materials, a roughness-induced increase in the effective adhesion energy can be observed for small roughness amplitudes, a result observed experimentally by Briggs and Briscoe.[17] It was also shown that stronger roughness is able to almost completely remove the adhesive bond, as observed in the classical paper by Fuller and Tabor.[18]

The case of an elastic plate in contact with a randomly rough substrate has been treated by one of us for full contact conditions,[2] and in this paper we extend the treatment to the case of partial contact. The problem under consideration is of great practical importance for understanding the adhesion of flies, bugs, and lizards to a rough substrate,[19,20] or the adhesive behavior of recently biologically-inspired adhesive films.[21] In the paper we consider in detail the case of a thin plate in partial contact with a hard substrate with a self-affine fractal rough surface. We assume that the plate deform according to linear elasticity theory, e.g., we assume that the stress in the film is everywhere below the yield stress of the material. We show that at large magnifications the plate can be regarded as an infinitely thick elastic slab, whereas, at small magnifications, because of its higher compliance, the plate is able to adhere in (apparent) full contact with the long wavelength feature of the rough substrate. This, in turn, produces a real contact area much larger than for the semi-infinite elastic solid. In other words, the repulsive elastic energy, produced by the plate deformation, will in many cases not be able to counterbalance the adhesion energy, resulting in a residual attractive macroscopic interfacial energy much larger than for the semi-infinite elastic solid.

This paper is organized as follows. In Sec. II we present a qualitative discussion of the importance of many length scales in adhesion. In Sec. III we review briefly the contact mechanics with adhesion and give expressions for the adhesion and elastic energies, and the effective interfacial energy γ_{eff}. In Sec. IV we present and discuss the numerical result obtained. In Sec. V we summarize the most important result, and in the Appendix we discuss briefly the contribution of the stretching energy of the plate.

II. QUALITATIVE DISCUSSION

Consider a thin elastic plate (thickness d) in frictionless contact with a corrugated rigid substrate. Let us estimate the change in the elastic energy needed to deform the plate, so that it goes in full contact with a substrate cavity of diameter λ and height h (we consider d/λ and h/λ sufficiently small). The bending elastic energy stored in the plate is $U_{el} \sim E\varepsilon^2\Delta V$ where $\varepsilon \sim hd/\lambda^2$ is the strain in the plate, and $\Delta V \sim \lambda^2 d$ is the volume where the elastic energy is stored. We get

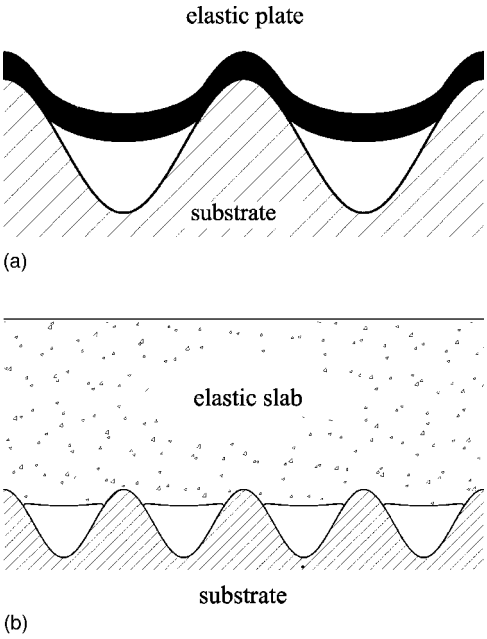

FIG. 1. (a) When the wavelength of the surface roughness is much longer than the thickness of the elastic slab, the plate is able to partially follow the substrate profile. (b) When the thickness of the slab is larger than the wavelength of the substrate the upper surface of the plate remains nearly flat.

$$(U_{el})_P \sim Ed^3\left(\frac{h}{\lambda}\right)^2. \tag{1}$$

If, instead of a thin plate, we consider a semi-infinite elastic solid, the strain is $\sim h/\lambda$, and the volume where the elastic displacement field is localized is $\sim\lambda^3$, giving

$$(U_{el})_S \sim E\lambda^3\left(\frac{h}{\lambda}\right)^2. \tag{2}$$

If $d \ll \lambda$ the elastic energy stored in plate is much smaller than the elastic energy stored in a semi-infinite elastic solid. Hence, the plate is elastically much softer than the semi-infinite elastic solid, and may be able to partially follow the substrate profile as shown in Fig. 1(a). When $d > \lambda$, Eq. (1) is not valid, and the plate will behave as a very thick elastic slab, and its upper surface will not be able to follow the substrate profile. This is illustrated in Fig. 1(b). Since for $d > \lambda$ the displacement field decays as $\exp(-2\pi z/\lambda)$ (z is the distance away from the substrate); the upper surface of the slab remains nearly flat. This is analogous to what happens to thin wetting films on rough surfaces.[22]

The change in the adhesion energy upon complete contact with the considered cavity is

$$U_{ad} \sim -\Delta\gamma\lambda^2, \tag{3}$$

where $\Delta\gamma = \gamma_1 + \gamma_2 - \gamma_{12}$ is the change of the surface energy per unit area due to the interaction between the elastic-solid and the substrate. We define the adhesion parameters θ_P and θ_S for the plate and the semi-infinite elastic solid, respectively, as

$$\theta_P = \frac{Ed^3}{\Delta\gamma\lambda^2}\left(\frac{h}{\lambda}\right)^2 \sim \frac{(U_{el})_P}{U_{ad}}, \tag{4}$$

$$\theta_S = \frac{E\lambda}{\Delta\gamma}\left(\frac{h}{\lambda}\right)^2 \sim \frac{(U_{el})_S}{U_{ad}}. \tag{5}$$

It is clear that θ_P and θ_S represent the competition between the attractive adhesion energy and the restoring elastic energy, and control the adhesive capability of an elastic body. When both θ_P and $\theta_S \ll 1$, the elastic plate or the semi-infinite solid will be able to fill out the cavities and adhere in full contact to the substrate. If, on the contrary, θ_P, $\theta_S > 1$ only partial contact will occur. Observe that, since the $\theta_P/\theta_S = (d/\lambda)^3$, we expect the thin plate ($d/\lambda \ll 1$) to have a much higher capability to adhere to a rough surface than the semi-infinite elastic solid. This explains why in many biological systems, showing a high adhesive ability, as for example the gecko foot pad, a very thin leaf-like plate (spatula) is found at the end of each thin fiber: the plate can easily bend to follow the long-wave surface roughness profile (see Fig. 2).

Most surfaces have roughness on a wide range of length scales. For example, many real surfaces are nearly a self-affine fractal. In these cases the statistical properties of the surface are invariant under the transformation:

$$\mathbf{x} \to \mathbf{x}\zeta, \quad z \to z\zeta^H,$$

where $\mathbf{x} = (x, y)$ is the 2D position vector in the mean plane of the corrugated surface, and z is the perpendicular distance away from this plane. The Hurst exponent H of the fractal surface is related to the surface fractal dimension via the relation $D_f = 3 - H$, with $0 < H < 1$. For this type of surface a simple scaling relation can be found between the surface amplitude h and the length scale λ. Let h_a be the surface amplitude at the reference length scale λ_a; then the amplitude h of the rough profile at the length scale λ is of the order

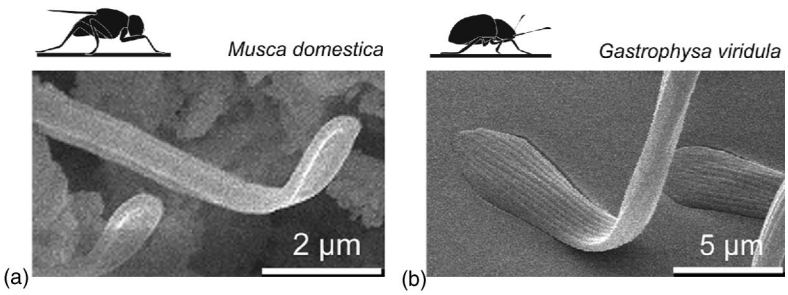

FIG. 2. Insect attachment system. Leaf-like element of the fiber in the fly *M. domestica*, A, and in the beetle *G. viridula*, B (from Refs. 2 and 27).

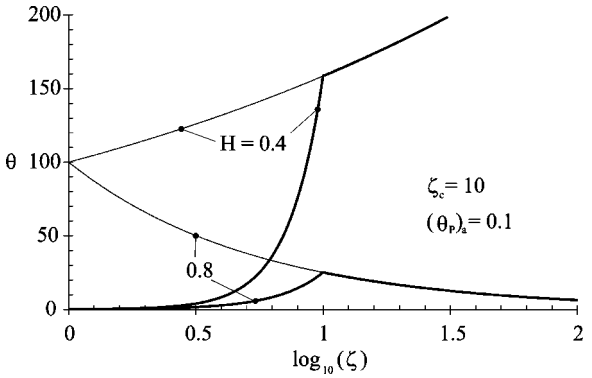

FIG. 3. The adhesive parameter θ as a function of the logarithm of the magnification ζ. The thick and thin lines correspond to the plate (θ_P) and the semi-infinite solid (θ_S) respectively.

$$\frac{h}{h_a} \sim \left(\frac{\lambda}{\lambda_a}\right)^H = \zeta^{-H}, \tag{6}$$

where we have introduced the magnification $\zeta = \lambda_a/\lambda$. Now suppose that at the reference length scale λ_a the thickness of the elastic slab is $d \ll \lambda_a$. Let us define the magnification ζ_c:

$$\zeta_c = \frac{\lambda_a}{d}. \tag{7}$$

At wavelengths smaller than d, that is $\zeta > \zeta_c$, the elastic slab can be regarded as a semi-infinite solid. We define the adhesion parameter θ_P for the elastic plate by means of the following relation:

$$\theta_P = \begin{cases} (\theta_P)_a \zeta^{2(2-H)}, & \zeta < \zeta_c, \\ \zeta_c^3 (\theta_P)_a \zeta^{1-2H}, & \zeta > \zeta_c, \end{cases} \tag{8}$$

where

$$(\theta_P)_a = \frac{Ed^3}{\Delta\gamma\lambda_a^2}\left(\frac{h_a}{\lambda_a}\right)^2.$$

Figure 3 compares the value of the adhesion parameters θ_P (plate) and θ_S (semi-infinite solid) for two different values of the Hurst exponent H. It is clear that at large wavelength, $\lambda \gg d$, that is $\zeta \ll \zeta_c$, the adhesion parameter is $\theta_P \ll 1$, and the plate is able to fill out the large substrate cavities and adhere to it in apparent full contact. The semi-infinite solid, on the other hand, will touch the substrate only on a small fraction of the nominal contact area because of its very large adhesive parameter $\theta_S \gg 1$. In this case during pull-off, the elastic energy stored at the interface will be released to overcome the change in the surface energy, and, as a consequence, no adherence force will be detected.

At higher magnification $\zeta > \zeta_c$ the plate behaves as a semi-infinite solid, but Fig. 3 shows that two completely different scenarios may result, depending on the values of the Hurst exponent. If $H = 0.8$ a further reduction of the adhesive parameter will be achieved by increasing the magnification, whereas if $H = 0.4$ the adhesive parameter continuously increases. Thus, if $H > 0.5$ ($D_f < 2.5$), as the magnification increases the elastic energy stored at the interface becomes increasingly less important compared to the energy of adhesion, i.e. the solid becomes more and more compliant and may rest in full contact with the short length scale structure of the rough profile. On the other hand, if $H < 0.5$ ($D_f > 2.5$) the elastic energy which would be stored at the interface in order to allow full contact, rapidly increases: in this case only partial contact occurs at the interface between the solid and the fine scale surface roughness.

Here we must point out that the arguments, presented above, are strictly true only if the substrate has roughness in only one direction. In this case, assuming no friction at the interface, the bending of the plate will not generate any tensile stress inside the plate, and no stretching energy will be produced. For a two-dimensional roughness, the plate bending may be accompanied by stretching,[23] so that an additional restoring force due to stretching elastic energy should be added at the largest scales (at the shortest scales the plate behaves as semi-infinite solids and this contribution does not exist). However, this will not affect the basic physics of the problem and the results we present in this paper. In the Appendix we briefly discuss under which conditions this stretching energy becomes important.

III. CONTACT MECHANICS

In this section we present the physical model and the basic set of equations that will be used to study the contact of a thin plate on a randomly rough surface. The theory is based on the formalism developed in Refs. 7 and 23; for the detailed derivations the readers are referred to these references.

A. The stress probability distribution and the apparent contact area

Consider the system at the length scale $\lambda = L/\zeta$, where L is the diameter of the nominal contact area, and define the wave vector $q = 2\pi/\lambda$. The smallest wave vector is $q_L = 2\pi/L$, and the magnification can be written as $\zeta = q/q_L$. Now let σ be the normal stress at the interface, and $P(\sigma, \zeta)$ the stress probability distribution in the contact area at the magnification ζ. $P(\sigma, \zeta)$ satisfies the following diffusion equation:[7,24]

$$\frac{\partial P}{\partial \zeta} = f(\zeta)\frac{\partial^2 P}{\partial \sigma^2}, \tag{9}$$

with the initial and boundary conditions

$$P(\sigma, 1) = \delta(\sigma - \sigma_0),$$

$$P(-\sigma_a, \zeta) = 0, \tag{10}$$

$$P(\infty, \zeta) = 0.$$

Here $\sigma_a(\zeta)$ is the tensile stress needed to cause detachment over an area of diameter $\lambda = L/\zeta$. $f(\zeta) = G'(\zeta)\sigma_0^2$ is a function of the magnification, and σ_0 denotes the average normal stress in the contact area. $G'(\zeta)$ is the ζ-derivative of the function

$$G(\zeta) = \pi\sigma_0^{-2}\int_{q_L}^{\zeta q_L} qM_{zz}(\mathbf{q})^{-1}M_{zz}(-\mathbf{q})^{-1}C(q)dq. \quad (11)$$

The quantity $M_{zz}(\mathbf{q})$ links the Fourier transform $\tilde{u}(\mathbf{q})$ of the normal displacement field $u(\mathbf{x})$ to the Fourier transform $\tilde{\sigma}(\mathbf{q})$ of the normal stress field $\sigma(\mathbf{x})$ at the interface:

$$\tilde{u}(\mathbf{q}) = M_{zz}(\mathbf{q})\tilde{\sigma}(\mathbf{q}). \quad (12)$$

We will derive an expression for M_{zz} in the next section. The surface roughness power spectra is

$$C(q) = \frac{1}{(2\pi)^2}\int \langle h(\mathbf{x})h(0)\rangle e^{-i\mathbf{q}\cdot\mathbf{x}}d^2x, \quad (13)$$

where $h(\mathbf{x})$ is the height of the rough profile above the mean plane of the surface. For a self-affine fractal surface the power spectra is given by

$$C(q) = \frac{H}{2\pi}\left(\frac{h_0}{q_0}\right)^2\left(\frac{q}{q_0}\right)^{-2(H+1)}, \quad (14)$$

where q_0 is the long-wave cut off vector, and h_0 is determined by the rms roughness amplitude $\langle h^2\rangle = h_0^2/2$ of the surface.

If $A(\zeta)$ denote the area of real contact (projected on the xy-plane) when the system is observed at the magnification $\zeta = L/\lambda$, then we define $P(\zeta) = A(\zeta)/A_0$ [where $A_0 = A(1)$ is the nominal contact area]. One can show that

$$P(\zeta) = \int_{-\sigma_a}^{\infty} P(\sigma,\zeta)d\sigma.$$

Solving Eq. (9) with the conditions Eq. (10), one obtains[7]

$$P(\zeta) = 1 - \int_1^{\zeta} d\zeta' S(\zeta'), \quad (15)$$

where $S(\zeta)$ can be calculated from the integral equation

$$\int_1^{\zeta} d\zeta' S(\zeta')\left[\frac{a(\zeta)}{a(\zeta)-a(\zeta')}\right]^{1/2}\exp\left\{-\frac{[\sigma_a(\zeta)-\sigma_a(\zeta')]^2}{4[a(\zeta)-a(\zeta')]}\right\} = \exp\left\{-\frac{[\sigma_a(\zeta)+\sigma_0]^2}{4a(\zeta)}\right\}, \quad (16)$$

with

$$a(\zeta) = \int_1^{\zeta} d\zeta' f(\zeta'). \quad (17)$$

B. Diffusivity function $f(\zeta)$

In this section we will derive an expression for $a(\zeta)$ which varies smoothly between the thin-film and the semi-infinite solid case. Since most real surfaces (and of course all self-affine fractal surfaces) have roughness over many decades of length scales, we believe that interpolating between the bulk and thin film limiting cases is highly accurately in the present application, since the wavelength region where the interpolation may not be so accurate is very small compared to the total range of wavelength involved in the adhesion problem.

For a semi-infinite elastic solid it has been shown[24] that $[M_{zz}^{-1}(\mathbf{q})]_S = Eq/[2(1-\nu^2)]$, but here we must calculate this quantity for the thin plate case. The equilibrium equation that governs the weak bending of an elastic thin plate is[23]

$$\frac{d^3}{12}\frac{E}{1-\nu^2}(\nabla^2)^2 u = \sigma \quad (18)$$

By Fourier transforming this equation one gets

$$[M_{zz}^{-1}(\mathbf{q})]_P = \frac{Eq}{2(1-\nu^2)}\frac{(qd)^3}{6}, \quad (19)$$

and for $f_P(\zeta)$,

$$f_P(\zeta) = G_P'(\zeta)\sigma_0^2 = \frac{\pi}{4}\left(\frac{Eq}{1-\nu^2}\right)^2 q_L q^3\left(\frac{q^3d^3}{6}\right)^2 C(q). \quad (20)$$

This should be compared with the result for a semi-infinite solid:

$$f_S(\zeta) = G_S'(\zeta)\sigma_0^2 = \frac{\pi}{4}\left(\frac{Eq}{1-\nu^2}\right)^2 q_L q^3 C(q). \quad (21)$$

The diffusivity function $f(\zeta)$ enables us to calculate the quantity $a(\zeta)$. For a self-affine fractal surface, Eq. (17) gives, for the thin plate and the semi-infinite solid, respectively,

$$a_P(\zeta) = \frac{1}{16}q_0^2h_0^2H\left(\frac{E}{1-\nu^2}\right)^2\left(\frac{q_0^3d^3}{6}\right)^2\frac{\zeta^{2(4-H)}-1}{4-H}, \quad (22)$$

$$a_S(\zeta) = \frac{1}{16}q_0^2h_0^2H\left(\frac{E}{1-\nu^2}\right)^2\frac{\zeta^{2(1-H)}-1}{1-H}. \quad (23)$$

Since at large magnification the plate behaves as a semi-infinite elastic solid, we can interpolate smoothly between the relations Eqs. (22) and (23) by using the expression

$$a(\zeta) = \left(\frac{q_0h_0}{4}\right)^2\left(\frac{E}{1-\nu^2}\right)^2 \times \frac{H(q_0d)^6(\zeta^{2(4-H)}-1)(\zeta^{2(1-H)}-1)}{36[(4-H)(\zeta^{2(1-H)}-1)]+(q_0d)^6(1-H)(\zeta^{2(4-H)}-1)}. \quad (24)$$

C. Detachment stress σ_a

It is clear that to solve the integral equation (16), we need to know the detachment stress $\sigma_a(\zeta)$. Let us, for the case of a thin plate, calculate the stress required to generate a detached zone of diameter λ. For a circular plate of radius $\lambda/2$ under the action of a uniform applied stress σ, the displacement field in the normal direction can be obtained from Eq. (18) and is given by[23]

$$u = \frac{3}{16}\frac{1-\nu^2}{Ed^3}\sigma\left(\frac{\lambda^2}{4}-r^2\right)^2. \quad (25)$$

Here we have assumed that $u'(\lambda/2) = 0$. The elastic energy required to deform the plate can be calculated as

$$U_{el} = \int \frac{1}{2} p u(r) d^2x = \frac{\pi}{2048} \frac{1-\nu^2}{Ed^3} \sigma^2 \lambda^6. \quad (26)$$

In order to evaluate the detachment stress σ_a, we require that the total energy $U_{\rm tot} = -\pi\gamma_{\rm eff}\lambda^2/4 + U_{el}$ has a minimum, so that

$$(\sigma_a)_P = \left[\frac{E\gamma_{eff}(\zeta)q}{2(1-\nu^2)}\right]^{1/2} \left(\frac{64}{3\pi^4} d^3q^3\right)^{1/2}, \quad (27)$$

where we have introduced the effective interfacial energy $\gamma_{\rm eff}$ (see Sec. III D). For the semi-infinite solid case, one obtains

$$(\sigma_a)_S = \left[\frac{E\gamma_{eff}(\zeta)}{1-\nu^2}\frac{q}{2}\right]^{1/2}, \quad (28)$$

and we can interpolate smoothly by using the following expression for the detachment stress:

$$\sigma_a(\zeta) = \left[\frac{E\gamma_{eff}(\zeta)q}{2(1-\nu^2)}\right]^{1/2} \left(\frac{d^3q^3}{3\pi^4/64 + d^3q^3}\right)^{1/2}. \quad (29)$$

D. Elastic energy and effective energy of adhesion

The detachment stress defined above depends on the value of the effective interfacial energy $\gamma_{\rm eff}$, which is a measure of the change in the plate free energy per unit area upon the contact with the substrate. Thus when the system is studied at the magnification ζ_a (see also Ref. 7 for a detailed treatment), the effective interfacial energy $\gamma_{\rm eff}(\zeta_a)$ is defined as

$$-\gamma_{eff}A(\zeta_a) = -\gamma_{eff}A_0P(\zeta_a) = U_{ad}(\zeta_a) + U_{el}(\zeta_a). \quad (30)$$

Thus, in order to evaluate $\gamma_{\rm eff}$ we must calculate the elastic energy of the system and the adhesion energy. For the plate case the elastic energy can be written as[23]

$$(U_{el})_P = \frac{Ed^3}{24(1-\nu^2)} \int d^2x \times \left\{ \langle(\nabla^2 u)^2\rangle - 2(1-\nu)\left\langle \frac{\partial^2 u}{\partial x^2}\frac{\partial^2 u}{\partial y^2} - \left(\frac{\partial^2 u}{\partial x \partial y}\right)^2 \right\rangle \right\}. \quad (31)$$

Now assume first that the plate makes contact everywhere with the substrate, so that $u(\mathbf{x}) = h(\mathbf{x})$. By using the definition of the inverse Fourier transform of the height substrate profile:

$$h(\mathbf{x}) = \int d^2q \tilde{h}(\mathbf{q}) e^{i\mathbf{q}\cdot\mathbf{x}},$$

we get

$$(U_{el})_P = \frac{A_0E}{24(1-\nu^2)} \int d^2q (qd)^3 qC(q), \quad (32)$$

where we have used that

$$\langle \tilde{h}(\mathbf{q})\tilde{h}(-\mathbf{q})\rangle = \frac{A_0}{(2\pi)^2} C(q).$$

At large magnification the plate behaves as an elastic semi-infinite solid where the elastic energy is[25]

$$(U_{el})_S = \frac{A_0E}{4(1-\nu^2)} \int d^2q q C(q). \quad (33)$$

We can interpolate smoothly between (32) and (33) by means of the following formula:

$$U_{el} = \frac{A_0E}{4(1-\nu^2)} \int d^2q C(q) q \frac{q^3d^3}{6+q^3d^3}. \quad (34)$$

For partial contact, we get

$$U_{el} = \frac{2\pi E}{4(1-\nu^2)} A_0 \int_{q_a}^{q_1} d^2q P(q) C(q) q^2 \frac{q^3d^3}{6+q^3d^3}. \quad (35)$$

Now let us give an expression for the adhesion energy U_{ad}. Consider first the plate adhered in (frictionless) full contact to the substrate. In this case the total area of contact equals the area[26] A_0 of the undeformed plate (note: when the plate is in full contact the contact area projected on the xy-plane is smaller than A_0), and the total energy of adhesion is

$$(U_{ad})_P = -A_0\Delta\gamma. \quad (36)$$

On the other hand when an elastic semi-infinite solid is considered to adhere in full contact to the substrate, the apparent contact area does not change, and the real area of contact A is larger than A_0. In this case the adhesion energy is[7,25]

$$(U_{ad})_S = -A_0\Delta\gamma \int_0^\infty (1+x\xi_S^2)^{1/2} e^{-x} dx, \quad (37)$$

where

$$\xi_S^2 = \int d^2q C(q) q^2.$$

In order to take into account that the plate behaves as a semi-infinite elastic solid at large magnifications we should interpolate between the two formulas. To perform this interpolation note that the elastic displacement vector field in the plate decreases as $\exp(-qz)$, so that, when the system is studied at the magnification $\zeta_a = q_a/q_L$, we can write

$$\xi^2 = 2\pi \int_{q_a}^{q_1} dq C(q) q^3 (1 - e^{-qd}). \quad (38)$$

Thus, by accounting for partial contact, the energy of adhesion at the magnification ζ_a is

$$U_{ad}(\zeta_a) = -A_0\Delta\gamma P(\zeta_1) \int_0^\infty (1+x\xi^2)^{1/2} e^{-x} dx, \quad (39)$$

and, by recalling Eq. (30), we get for the effective interfacial energy,

$$\frac{\gamma_{eff}}{\Delta\gamma} = \frac{P(\zeta_1)}{P(\zeta_a)} \int_0^\infty (1+x\xi^2)^{1/2} e^{-x} dx - \frac{2\pi}{\delta} \int_{q_a}^{q_1} d^2q \frac{P(q)}{P(q_a)} C(q) q^2 \frac{q^3d^3}{6+q^3d^3}, \quad (40)$$

where we have introduced the adhesion length

$$\delta = 4(1-\nu^2)\Delta\gamma/E. \quad (41)$$

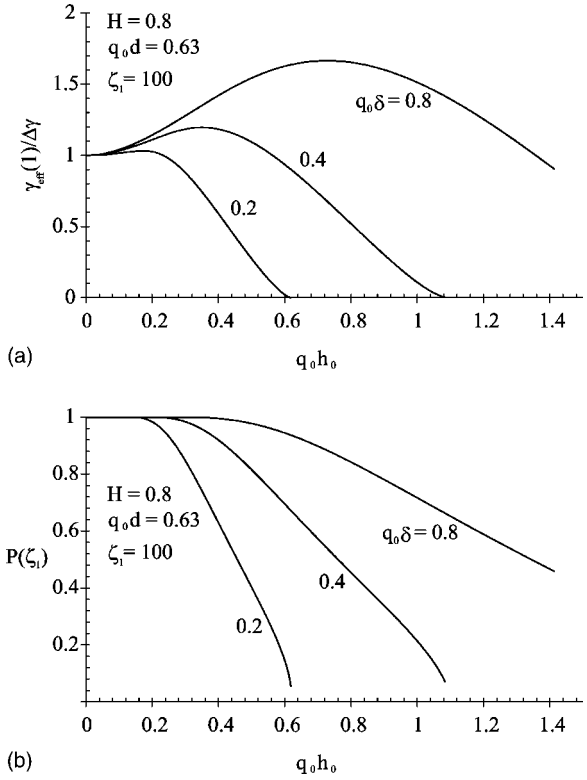

FIG. 4. (a) The normalized macroscopic interfacial energy $\gamma_{eff}(\zeta=1)/\Delta\gamma$ and (b) the normalized area of real contact, $P(\zeta_1)=A(\zeta_1)/A_0$ as a function of the dimensionless surface amplitude q_0h_0. Results are shown for $H=0.8$, $\zeta_1=100$, $q_0d=0.63$, and for different values of $q_0\delta$.

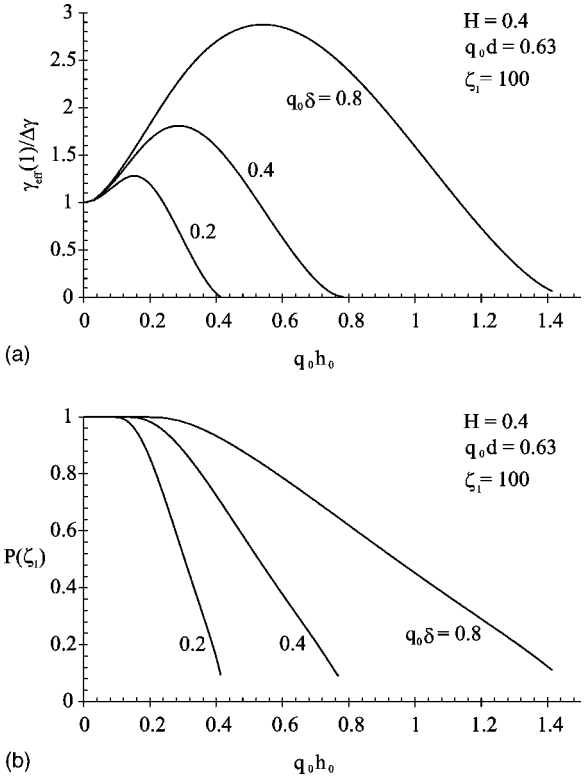

FIG. 5. (a) The normalized macroscopic interfacial energy $\gamma_{eff}(\zeta=1)/\Delta\gamma$ and (b) the normalized area of real contact, $P(\zeta_1)=A(\zeta_1)/A_0$ as a function of the dimensionless surface amplitude q_0h_0. Results are shown for $H=0.4$, $\zeta_1=100$, $q_0d=0.63$, and for different values of $q_0\delta$.

IV. RESULTS AND DISCUSSION

Equations (15), (16), (29), and (40) can be solved by an iterative numerical procedure. In this section we present results for a surface which is a self-affine fractal on all length scales, i.e., $q_L=q_0$. The calculations have been performed for two values of the Hurst exponent, $H=0.8$ and $H=0.4$, and for a maximum magnification $\zeta_1=q_1/q_0=100$. The effective adhesion energy $\gamma_{eff}(\zeta)$ and the normalized area of contact $P(\zeta)$ are compared to the those obtained for the semi-infinite elastic solid.

Figure 4 shows (a) the macroscopic interfacial energy $\gamma_{eff}(1)$, i.e. the effective interfacial energy calculated at the magnification $\zeta=1$, and (b) the normalized area of real contact $P(\zeta_1)$ at the maximum magnification $\zeta=\zeta_1$, as a function of the dimensionless roughness amplitude q_0h_0. We show results for three different values of $q_0\delta$, where the adhesion length δ is defined by Eq. (41). The results are plotted for $H=0.8$, i.e. $D_f=2.2$, and for a dimensionless thickness of the plate equal to $q_0d=0.63$. Note that the macroscopic interfacial energy initially increases with the amplitude h_0 of the rough profile up to a maximum value, and after decreases with h_0. This is caused by the increase in the real contact area produced by the fine structure of the rough profile. Figure 4(b) shows, indeed, that at small h_0 the plate adheres in full contact to the substrate, so that an increase in the surface roughness produces a corresponding increases of the area of contact and, hence, of the surface energy. However this is no more true at large h_0, because of the reduction of the area of real contact. Figure 4 also shows that, as expected, the roughness-induced increment of the macroscopic interfacial energy grows by increasing the adhesion length $\delta\sim\Delta\gamma/E$, and that the full contact condition remains to higher amplitude h_0 as δ increases.

In Fig. 5 we report the same quantities as in Fig. 4 but for a smaller Hurst exponent $H=0.4$ (fractal surface dimension $D_f=2.6$). In this case the enhancement in the macroscopic interfacial energy is much larger than for $H=0.8$. This result is expected since, when the plate adheres in full contact with the substrate, the roughness-induced increase in the contact area is larger for a higher surface fractal dimension. This, in turn, increases the adhesive contribution to the interfacial energy. However, we also observe that at high enough amplitudes h_0 both the macroscopic interfacial energy and the real contact area decrease much faster than for $H=0.8$. This result is expected since the adhesion parameter θ given by Eq. (8) always increases as the fractal dimension $D_f=3-H$ of the surface increases. This implies that when only partial contact occurs (large enough q_0h_0 values), the area of real contact will be much smaller for $H=0.4$ than for $H=0.8$, and the macroscopic interfacial energy will be significantly reduced.

Figures 6 and 7 compare the results obtained for the plate case (thick lines) with those of the semi-infinite solid (thin lines), for $H=0.8$ and $H=0.4$. As expected, because of the

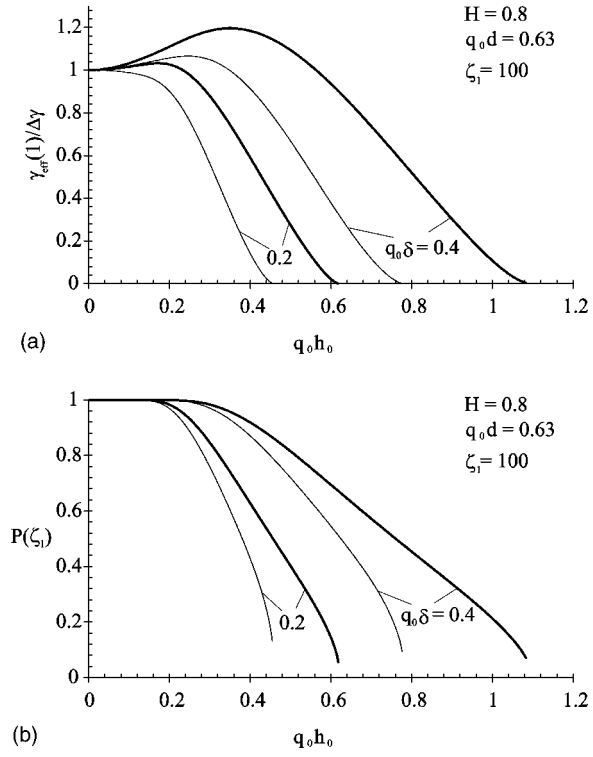

FIG. 6. (a) The normalized macroscopic interfacial energy $\gamma_{eff}(\zeta=1)/\Delta\gamma$ and (b) the normalized area of real contact, $P(\zeta_1)=A(\zeta_1)/A_0$, as a function of the dimensionless surface amplitude q_0h_0. Thick lines are for the plate case and thin lines are for the semi-infinite solid case. Results are shown for $H=0.8$, $\zeta_1=100$, $q_0d=0.63$, and for two different values of $q_0\delta$.

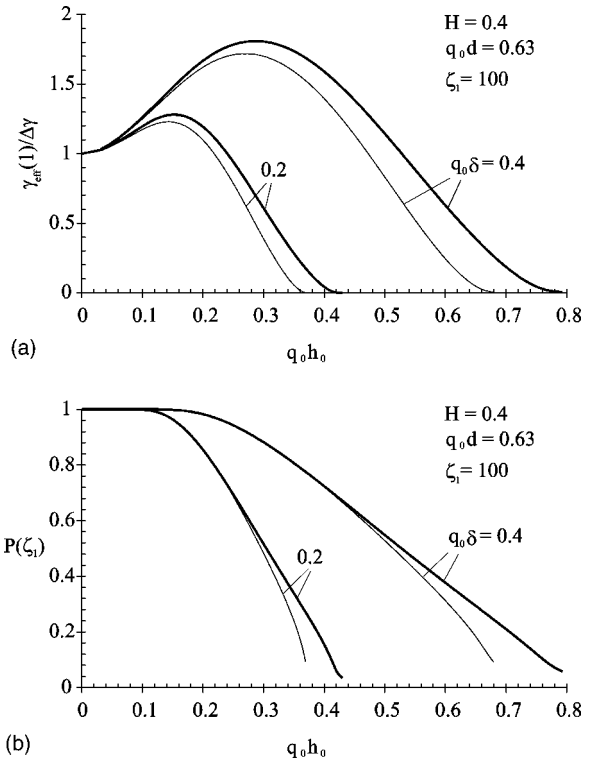

FIG. 7. (a) The normalized macroscopic interfacial energy $\gamma_{eff}(\zeta=1)/\Delta\gamma$ and (b) the normalized area of real contact, $P(\zeta_1)=A(\zeta_1)/A_0$, as a function of the dimensionless surface amplitude q_0h_0. Thick lines are for the plate case and thin lines are for the semi-infinite solid case. Results are shown for $H=0.4$, $\zeta_1=100$, $q_0d=0.63$, and for two different values of $q_0\delta$.

higher compliance of the plate, both the macroscopic interfacial energy $\gamma_{eff}(1)$ and the normalized area of real contact $P(\zeta_1)$ are larger than for the semi-infinite solid case. However, for $H=0.4$ this difference is less significant (see Fig. 7). This can be easily understood if we consider that for $H=0.4$ the adhesive parameter θ rapidly increases (see Fig. 3) with the magnification ζ: the small scale roughness contribution is now much more important than for $H=0.8$. Thus when $H<0.5$ the long wave-length contribution to the macroscopic interfacial energy is less significant, and the plate behavior is much closer to that of a semi-infinite solid.

Figure 8 shows (a) the normalized effective energy of adhesion, and (b) the normalized (apparent) area of contact $P(\zeta)$ as a function of the logarithm of the magnification ζ. The plate results (solid lines) are compared with those of the semi-infinite elastic solid (thin lines) for $H=0.8$ and $H=0.4$. The curves have been plotted for the dimensionless plate thickness $q_0d=0.63$, that is for $\zeta_c=\lambda_0/d\simeq 10$. Therefore, we expect that for $\log_{10}\zeta>1$ no appreciable differences should be noticed in comparison to the semi-infinite solid case. Indeed, Fig. 8(a) shows that the thick and thin curves cannot be distinguished when $\log_{10}\zeta>1$. On the other hand, at smaller magnifications the influence of the higher plate compliance is clearly seen, and the macroscopic interfacial energy $\gamma_{eff}(\zeta=1)$ is much larger for the plate than for the semi-infinite solid.

Note also that at short length scales, $\gamma_{eff}(\zeta)$ increases with decreasing magnification. This effect is due to the increase in the contact area as more and more short-wavelength roughness components are "integrated-out." However at small enough magnifications the contribution to the interfacial energy from the roughness-induced elastic energy leads to a reduction of the effective adhesion energy.

Figure 8(b) also shows that for $\zeta>\zeta_c\simeq 10$ the slope of the $P(\zeta)$ curves does not appreciably vary when considering the thin plate or the semi-infinite solid. However, because of the cumulative nature of $P(\zeta)$, the contact area of the plate is larger than that of the semi-infinite solid over the whole ζ-range. This is a consequence of the higher plate compliance at small magnification, which allows for an apparent full contact condition up to much larger values of ζ. Observe, additionally, that for $H=0.8>0.5$, the normalized area of contact $P(\zeta)$ reaches a constant value as the magnification is increased, i.e. the plate adheres in full contact to the short length scale structure of the rough surface. On the other hand, when $H=0.4<0.5$, the normalized area of contact $P(\zeta)$ continuously decreases with increasing magnification ζ. This confirms the qualitative results of Sec. II obtained by means of scaling law considerations. Moreover, Fig. 8(a) shows that, in the transition zone where the plate behavior changes smoothly toward the semi-infinite solid characteristic behavior, the effective interfacial energy is smaller for the plate than for the semi-infinite solid. However, if we observe that the free energy of the plate is proportional to $-P(\zeta)\gamma_{eff}(\zeta)$, and considering that in the same zone the area of (apparent)

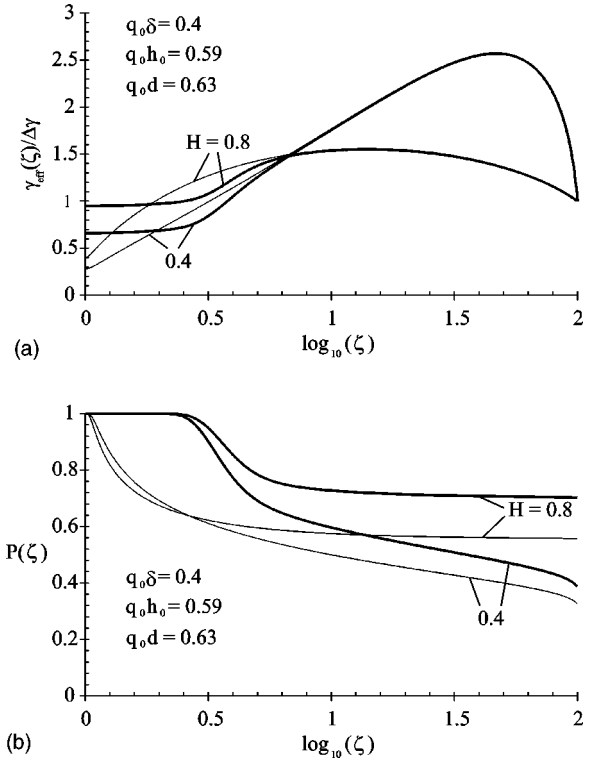

FIG. 8. (a) The normalized effective energy of adhesion $\gamma_{eff}(\zeta)/\Delta\gamma$ and (b) the normalized (apparent) area of contact $P(\zeta) = A(\zeta)/A_0$ as a function of $\log_{10}(\zeta)$. Results are reported for two values $H=0.8$ and $H=0.4$ of the Hurst fractal exponent. Thick lines are for the plate case and thin lines are for the semi-infinite solid case.

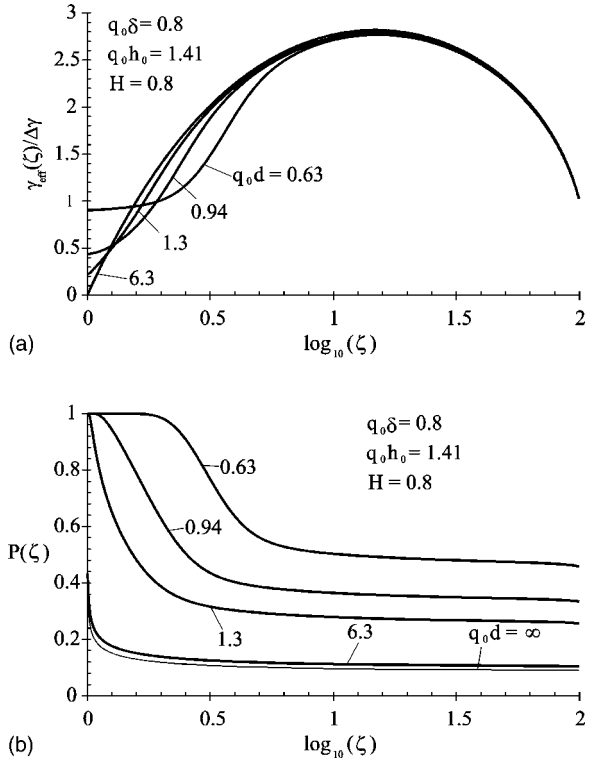

FIG. 9. (a) The normalized effective energy of adhesion $\gamma_{eff}(\zeta)/\Delta\gamma$ and (b) the normalized (apparent) area of contact $P(\zeta) = A(\zeta)/A_0$ as a function of $\log_{10}(\zeta)$. Results are reported for $H = 0.8$ and different values of the dimensionless thickness q_0d of the plate. Thick lines are for the plate case and thin lines are for the semi-infinite solid case.

contact is much larger for the plate than for the semi-infinite solid, we conclude that the total free energy of the plate is smaller than for the semi-infinite solid over the whole ζ-range.

Figure 9 shows (a) the normalized effective energy of adhesion and (b) the normalized (apparent) area of contact $P(\zeta)$ as a function of the logarithm of the magnification ζ, for different values of the dimensionless thickness of plate q_0d. It is clear that by increasing the thickness of the plate the curves approaches those corresponding to the semi-infinite solid case, and, as expected, when $q_0d=6.3$ (i.e., $d/\lambda \simeq 1$), no appreciable difference can be observed between the two cases.

V. CONCLUSION

We have studied the adhesion of a thin elastic plate to a randomly rough rigid substrate with self-affine fractal roughness. It has been shown that, because of its higher compliance, the plate may adhere in apparent full contact to the long-length scale structure of the rough substrate. This produces a larger area of real contact and a significantly higher effective energy of adhesion, in comparison to the semi-infinite elastic solid case. Thus, the plate adheres more strongly to the substrate, and this may justify why lizards, beetles, or spiders, all characterized by exceptionally high adhesive abilities, have a leaf-like plate structure at the end of the thin fibers (see Fig. 2), of which the foot-pad surface is made-up.

In the paper we also show that at length scales equal to or smaller than the plate thickness, no appreciable differences can be observed with the semi-infinite solid case. Thus, for example, in a typical case the plate will be able to rest in full contact with the fine structure of the rough surface only if the fractal dimension is close to 2, whereas only partial contact will occur for surface fractal dimension higher than 2.5.

APPENDIX: THE CONTRIBUTION OF STRETCHING ENERGY

In this section we present a short derivation of the stretching elastic energy produced by the bending of the plate. We assume that full contact occurs between the plate and substrate. Let us first estimate the elastic energy due to the stretching of the plate. Suppose that the plate is deformed so that it goes in full contact with a substrate cavity of diameter λ and height h. The stretching elastic energy is $U_s \sim E\varepsilon_s^2 \Delta V$ where $\varepsilon_s \sim (h/\lambda)^2$ and $\Delta V \sim \lambda^2 d$ is the volume where the elastic energy is stored. Thus we get

$$U_s \sim E\lambda^2 d\left(\frac{h}{\lambda}\right)^4. \tag{A1}$$

If we compare this quantity with the elastic energy due to the bending of the plate $U_b \sim Ed^3(h/\lambda)^2$ [see Eq. (1)], we find that

$$U_b/U_s \sim (d/h)^2. \tag{A2}$$

Thus, if $h > d$ the contribution of the stretching deformations of the plate can, in general, not be neglected. In this case the governing equations are[23]

$$\frac{E}{1-\nu^2}\frac{d^3}{12}(\nabla^2)^2 u - d\left(\frac{\partial^2\chi}{\partial y^2}\frac{\partial^2 u}{\partial x^2} + \frac{\partial^2\chi}{\partial x^2}\frac{\partial^2 u}{\partial y^2} - 2\frac{\partial^2\chi}{\partial x\partial y}\frac{\partial^2 u}{\partial x\partial y}\right) = \sigma, \tag{A3}$$

$$(\nabla^2)^2\chi + E\left[\frac{\partial^2 u}{\partial x^2}\frac{\partial^2 u}{\partial y^2} - \left(\frac{\partial^2 u}{\partial x\partial y}\right)^2\right] = 0, \tag{A4}$$

where u is the normal displacement field, σ is the normal stress acting on the plate, and χ is the stress function defined as

$$\sigma_{11} = \frac{\partial^2\chi}{\partial y^2},\ \ \sigma_{12} = -\frac{\partial^2\chi}{\partial x\partial y},\ \ \sigma_{22} = \frac{\partial^2\chi}{\partial x^2}. \tag{A5}$$

The stretching elastic energy can be calculated as

$$U_s = \frac{d}{2}\int d^2x \langle \varepsilon_{ij}(\mathbf{x})\sigma_{ij}(\mathbf{x})\rangle, \tag{A6}$$

where $\langle\cdots\rangle$ stands for the ensemble average, and σ_{ij} and ε_{ij} $(i,j=1,2)$ are the in-plane stress and strain tensors, respectively, related to each-other by the constitutive equations of elasticity:

$$\varepsilon_{11} = \frac{1}{E}(\sigma_{11} - \nu\sigma_{22}),$$

$$\varepsilon_{22} = \frac{1}{E}(\sigma_{22} - \nu\sigma_{11}), \tag{A7}$$

$$\varepsilon_{12} = \frac{1}{E}(1+\nu)\sigma_{12}.$$

By using Eqs. (A4), (A5), and (A7) we can derive an expression for the elastic energy as a function of the elastic displacement field. Let us define

$$\sigma_{ij}(\mathbf{x}) = \int d^2q \sigma_{ij}(\mathbf{q}) e^{i\mathbf{q}\cdot\mathbf{x}},$$

so that by using Eqs. (A7) we can express the elastic energy as

$$U_s = \frac{d}{2E}\int d^2q \{[\sigma_{11}(\mathbf{q}) - \nu\sigma_{22}(\mathbf{q})]\sigma_{11}(-\mathbf{q}) + [\sigma_{22}(\mathbf{q}) - \nu\sigma_{11}(\mathbf{q})]\sigma_{22}(-\mathbf{q}) + 2(1+\nu)\sigma_{12}(\mathbf{q})\sigma_{12}(-\mathbf{q})\}$$

Moreover, by means of Eqs. (A5) it is possible to find $\sigma_{ij}(\mathbf{q})$ as a function of $\chi(\mathbf{q})$, that in turn can be expressed in terms of $h(\mathbf{q})$ by means of Eq. (A4):

$$\chi(\mathbf{q}) = -\frac{E}{q^4}\int d^2q' h(\mathbf{q}')h(\mathbf{q}-\mathbf{q}')[q_x'^2(q_y - q_y')^2 - q_x'q_y'(q_x - q_x')(q_y - q_y')]$$

The stretching elastic energy is therefore

$$U_s = \frac{Ed}{2}(2\pi)^2\int d^2q d^2q' d^2q'' \times\langle h(\mathbf{q}')h(\mathbf{q}'')h(\mathbf{q}-\mathbf{q}')h(-\mathbf{q}-\mathbf{q}'')\rangle \times\frac{1}{q^4}f(\mathbf{q},\mathbf{q}')f(-\mathbf{q},\mathbf{q}''), \tag{A8}$$

where

$$f(\mathbf{q},\mathbf{q}') = q_x'(q_y - q_y')(q_x'q_y - q_xq_y').$$

Now observe that for a Gaussian random variable $h(\mathbf{q})$,

$$\langle h(\mathbf{q}')h(\mathbf{q}'')h(\mathbf{q}-\mathbf{q}')h(-\mathbf{q}-\mathbf{q}'')\rangle = \frac{A_0}{(2\pi)^2}C(\mathbf{q}')C(\mathbf{q}-\mathbf{q}') \times[\delta(\mathbf{q}'+\mathbf{q}'') + \delta(\mathbf{q}'-\mathbf{q}-\mathbf{q}'')] \tag{A9}$$

so that we can write

$$U_s = \frac{1}{4}A_0Ed\int d^2qd^2q'\frac{C(q)C(q')}{|\mathbf{q}+\mathbf{q}'|^4}(q_xq_y' - q_x'q_y)^4 = \frac{1}{4}A_0Ed\int d^2qd^2q' C(q)C(q')\frac{|\mathbf{q}\times\mathbf{q}'|^4}{|\mathbf{q}+\mathbf{q}'|^4},$$

where in the last equation we have defined $\mathbf{q}=(q_x,q_y,0)$. Introducing the polar coordinates gives

$$U_s = \frac{1}{4}A_0Ed\int dqdq' C(q)C(q')q^5q'^5 \times\int d\theta d\theta'\frac{\sin^4(\theta-\theta')}{[q^2+q'^2+2qq'\cos(\theta-\theta')]^2}.$$

Now, note that

$$\int d\theta d\theta'\frac{\sin^4(\theta-\theta')}{[q^2+q'^2+2qq'\cos(\theta-\theta')]^2} = g(q,q'),$$

where

$$g(q,q') = \frac{3\pi^2}{2}\times\begin{cases}1/q^4; & q \geqslant q',\\ 1/q'^4; & q < q'.\end{cases}$$

Therefore the stretching energy is

$$U_s = \frac{1}{4}A_0Ed\int dqdq' q^5q'^5 g(q,q')C(q)C(q'). \tag{A10}$$

For a self-affine rough surface, Eqs. (14) and (A10) give the following expression for the stretching energy:

$$U_s = \frac{Ed}{2} A_0 \frac{3}{64} (q_0 h_0)^4 \frac{H}{2-H} \frac{H\zeta_c^{4-4H} + 2(1-H)\zeta_c^{-2H} - (2-H)}{1-H}, \tag{A11}$$

where $\zeta_c = \lambda_0/d$ is the cut-off magnification corresponding to a wavelength $\lambda = d$. For magnifications $\zeta > \zeta_c$ the plate behaves as a semi-infinite solid and the stretching effect vanishes. Let us compare this energy with the bending energy of the plate [see Eq. (32)]:

$$U_b = \frac{1}{4(1-\nu^2)} \frac{Ed}{2} A_0 (q_0 h_0)^2 \frac{H}{2-H} \frac{q_0^2 d^2}{6} (\zeta_c^{4-2H} - 1). \tag{A12}$$

By taking the ratio, one gets

$$\frac{U_s}{U_b} = \frac{9}{8}(1-\nu^2)\left(\frac{h_0}{d}\right)^2 \frac{H\zeta_c^{4-4H} + 2(1-H)\zeta_c^{-2H} - (2-H)}{(1-H)(\zeta_c^{4-2H} - 1)} \approx \frac{9}{8}(1-\nu^2)\left(\frac{h_0}{d}\right)^2 \frac{H}{1-H}\zeta_c^{-2H}.$$

For the case considered in the paper we have $\zeta_c \sim 10$, $d/h_0 \sim 1$ so we get $U_s/U_b \simeq 0.1$. If we consider the gecko case, we have $d/h_0 \sim 0.25$, $\zeta_c = \lambda/d \sim 100$, and $U_s/U_b \simeq 0.02$, and the stretching contribution can be neglected. In general, we believe that the basic physics will not change when the influence of the stretching energy is included, but in a future publication we plan to consider the effect of the stretching energy also for the partial contact case.

[1] E. E. Jones, M. R. Begleyb, and K. D. Murphy, J. Mech. Phys. Solids **51**, 1601 (2003).

[2] S. N. Gorb, *Attachment Devices of Insect Cuticle* (Kluwer Academic, Dordrecht, 2001); see also M. Scherge and S. Gorb, *Biological Micro- and Nano-Tribology* (Springer-Verlag, Berlin, 2001).

[3] L. P. B. Katehi, J. F. Harvey, and E. Brown, IEEE Trans. Microwave Theory Tech. **50**, 858 (2002).

[4] N. P. Padture, M. Gell, and E. H. Jordan, Science **296**, 280 (2002).

[5] L. D. Piveteau, B. Gasser, and L. Schlapbach, Biomaterials **21**, 2193 (2000).

[6] K. T. Turner and S. M. Spearing, J. Appl. Phys. **92**, 7658 (2002).

[7] B. N. J. Persson, Eur. Phys. J. E **8**, 385 (2002); Eur. Phys. J. E **89**, 245502 (2002).

[8] B. N. J. Persson, *Sliding Friction: Physical Principles and Applications*, 2nd ed. (Springer-Verlag, Heidelberg, 2000).

[9] G. Carbone and L. Mangialardi, J. Mech. Phys. Solids **52**, 1267–1287 (2004).

[10] H. Yoshizawa, Y. Chen, and J. Israelachvili, J. Phys. Chem. **97**(16), 4128 (1993).

[11] H. Yoshizawa and J. Israelachvili, J. Phys. Chem. **97**, 11300 (1993).

[12] B. Bhushan, J. N. Israelachvili, and U. Landman, Nature (London) **374**, 607 (1995).

[13] J. N. Israelachvili, *Intermolecular and Surface Forces* (Academic, London, 1995).

[14] N. Maeda, N. Chen, M. Tirrel, and J. N. Israelachvili, Science **297**, 379 (2002).

[15] S. Zilberman and B. N. J. Persson, Solid State Commun. **123**, 173 (2002); **124**, 227 (2002), J. Chem. Phys. **118**, 6473 (2003).

[16] G. Carbone and P. Decuzzi, J. Appl. Phys. **95**, 4476 (2004).

[17] G. A. D. Briggs and B. J. Briscoe, J. Phys. D **10**, 2453 (1977).

[18] K. N. G. Fuller and D. Tabor, Proc. R. Soc. London, Ser. A **345**, 327 (1975); see also K. L. Johnson, *The Mechanics of the Contact Between Deformable Bodies*, edited by A. D. de Pater and J. J. Kalker (Delft University of Technology, the Netherlands, Sijthoff & Noordhoff Int. Pub., Hardbound, 1975), and D. Maugis, *Contact Adhesion and Rupture of Elastic Solids* (Springer-Verlag, Berlin, 2000).

[19] S. Gorb and B. N. J. Persson, J. Chem. Phys. **119**, 11437 (2003).

[20] B. N. J. Persson, J. Chem. Phys. **118**, 7614 (2003).

[21] A. K. Geim, S. V. Dubonos, I. V. Gricorieva, K. S. Novoselov, A. A. Zhukov, and S. Yu. Shapoval, Nat. Mater. **2**, 461 (2003).

[22] M. O. Robbins, D. Andelman, and J. F. Joanny, Phys. Rev. A **43**, 4344 (1991).

[23] L. D. Landau and E. M. Lifshitz, *Theory of Elasticity* (Pergamon, London, 1959).

[24] B. N. J. Persson, J. Chem. Phys. **115**, 3840 (2001).

[25] B. N. J. Persson and E. Tosatti, J. Chem. Phys. **115**, 5597 (2001).

[26] Observe that this statement is rigorously true only if the corrugated substrate has roughness in only one direction. For two dimensional roughness the bending often produces stretching of the plate, that, in turn, will result in an increased total contact area.

[27] A. G. Peressadko and S. N. Gorb, J. Adhes. **80**(4), 247 (2004).